DC magnetic susceptibility and neutron powder diffraction analysis of the perovskite-type compounds $LaYbO_3$ and $LaHoO_3$

2013 J. Phys.: Condens. Matter 25 426005

(http://iopscience.iop.org/0953-8984/25/42/426005)

J. Phys.: Condens. Matter **25** (2013) 426005 (7pp) doi:10.1088/0953-8984/25/42/426005

DC magnetic susceptibility and neutron powder diffraction analysis of the perovskite-type compounds $LaYbO_3$ and $LaHoO_3$

A Martinelli[1], R Masini[2], C Artini[3,4], G A Costa[4] and L Keller[5]

[1] CNR-SPIN, Corso Perrone 24, I-16152 Genova, Italy
[2] CNR-IMEM, Via Dodecaneso 33, I-16146 Genova, Italy
[3] CNR-IENI, Via de Marini 6, I-16149 Genova, Italy
[4] Department of Chemistry and Industrial Chemistry, University of Genova, Via Dodecaneso 31, I-16146 Genova, Italy
[5] Paul Scherrer Institut, 5232 Villigen PSI, Switzerland

E-mail: alberto.martinelli@spin.cnr.it

Received 21 February 2013, in final form 1 July 2013
Published 30 September 2013
Online at stacks.iop.org/JPhysCM/25/426005

Abstract
Magnetization measurements and neutron powder diffraction analyses followed by Rietveld refinement have been carried out in order to investigate the magnetic structures of $LaYbO_3$ and $LaHoO_3$. Both compounds exhibit a negative thermal expansion along the *a* and *b* axes. In $LaYbO_3$ Yb^{3+} spins order at 2.4 K according to a F_yG_z-type structure, belonging to the $Pn'ma'$ magnetic space group. Conversely, $LaHoO_3$ is paramagnetic down to 1.5 K.

(Some figures may appear in colour only in the online journal)

1. Introduction

$LaREO_3$ type oxides (RE ≡ Ho–Lu) constitute a rather unexplored class of materials, despite their interesting structural and magnetic features [1–3]. They are characterized by an orthorhombic perovskite-type structure, isostructural with $GdFeO_3$, distorted on account of the reduced value of the Goldschmidt tolerance factor (*t*) [4]. Such a distortion increases from Lu to Ho, i.e. increases with the RE size. Recently, a structural study on these compounds has been undertaken by our group [5] in order to investigate the possible correlation among the Goldschmidt factor *t*, the stability field extent as a function of temperature, and their magnetic properties. It has been found out that the larger is the deviation from the ideal case, the smaller is the extent of the stability field versus temperature, as also other structures typical of rare earths sesquioxides appear. Moreover, the decrease of the Curie–Weiss temperature θ with decreasing RE size points out a strengthening of the exchange interactions due to the shortening of the atomic distances.

At present only the magnetic structure of $LaErO_3$ has been studied using neutron powder diffraction (NPD) analysis, by Moreau *et al* in the late 1960s [6]; as a result, an antiferromagnetic (AFM) ordering was detected below 2.4 K, with an $A_xG_yC_z$-type arrangement of the Er spins and a total moment equal to 6.3 μ_B. More recently Ito *et al* [7] analysed the magnetic susceptibility of both $LaYbO_3$ and $LaHoO_3$, finding an AFM transition at 2.7 K for the former compound, with a weak ferromagnetic (FM) component related to Yb^{3+} spin canting. Conversely, $LaHoO_3$ was found to be paramagnetic (PM) down to 1.8 K.

In this work an analysis of the magneto-chemical properties of $LaYbO_3$ and $LaHoO_3$ is presented, as revealed by dc magnetic susceptibility measurements and neutron powder diffraction analysis.

2. Experimental details

Samples were prepared by thermal decomposition of the corresponding mixed oxalates, synthesized via a

coprecipitation method starting from powders of RE oxide (La_2O_3 99.99% MATECK; Yb_2O_3 99.9% ALDRICH; Ho_2O_3 99.9% ALDRICH) dissolved in HCl 13 vol%; the precipitation of the mixed oxalates was achieved by adding a solution of oxalic acid in large excess [5]. The precipitate was dried in air at 80 °C for 72 h, heated in air at 1200 °C for two days and finally quickly cooled in air.

The purity of the samples was checked by x-ray powder diffraction analysis (XRPD; PHILIPS PW1830; Bragg–Brentano geometry; Cu Kα; secondary monochromator; 2θ range: 15°–110°; step: 0.020° 2θ; sampling time: 12 s); Rietveld refinement was carried using the program FullProf [8]. The peak shape was modelled with a pseudo-Voigt convoluted with axial divergence asymmetry function coupled to an instrumental file. In the final cycle the following parameters were refined: the scale factor; the zero point of detector; the background (four parameters of the fifth-order polynomial function); the unit cell parameters; the atomic site coordinates not constrained by symmetry; the isotropic displacement parameter; the Lorentzian isotropic strain.

Neutron powder diffraction analysis (NPD; $\lambda = 2.4585$ Å; step = 0.1°) was carried out at the spallation neutron source SINQ of the Paul Scherrer Institute (Villigen, CH) using the high-intensity DMC diffractometer equipped with an Orange He cryostat. NPD patterns were acquired at 100 K, in PM state, and in the T range 1.5–5 K, where magnetic ordering is located, if present, for compounds belonging to this class of materials. For the Rietveld refinement the peak shape was modelled with a pseudo-Voigt function. In the final cycle the following parameters were refined: the scale factor; the zero point of detector; the background (fifth-order polynomial function); the unit cell parameters; the atomic site coordinates not constrained by symmetry; the overall isotropic displacement parameter; the magnetic moment at the octahedral site (when the magnetic scattering contribution is present).

The dc magnetic susceptibility of all the samples was measured with a SQUID magnetometer (Quantum Design MPMS) in the temperature range $T = 350$–1.8 K with an applied field of $H = 0.1$ T. No demagnetization correction was done in our magnetization measurements. Molar magnetic susceptibilities were calculated by applying diamagnetic corrections using Pascal's constants.

3. Results and discussion

3.1. Magnetic properties

Figures 1 and 2 show the thermal dependence of the inverse magnetic susceptibility (χ^{-1}) for $LaYbO_3$ and $LaHoO_3$, respectively.

The data of the inverse susceptibility at high temperature were fitted by the Curie–Weiss law

$$\chi = \frac{C}{(T-\theta)} \tag{1}$$

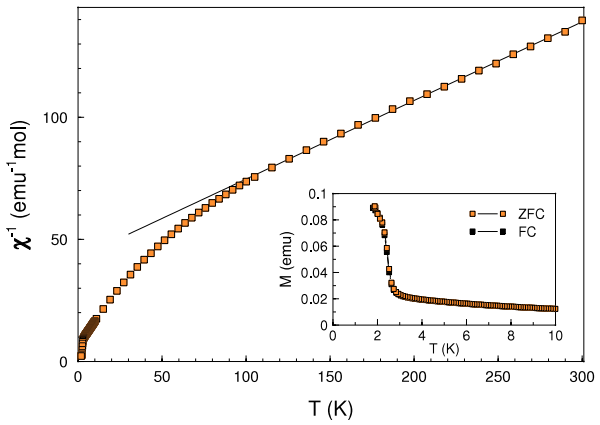

Figure 1. Thermal dependence of χ^{-1} for $LaYbO_3$; inset: low-temperature behaviour of magnetization M.

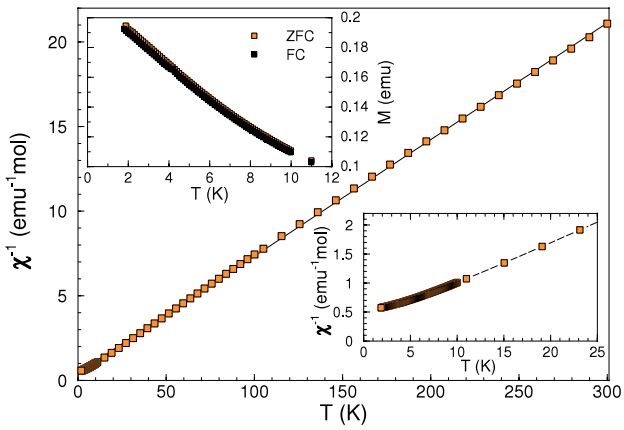

Figure 2. Thermal dependence of χ^{-1} for $LaHoO_3$; inset: low-temperature behaviour of magnetization M and χ^{-1}.

with

$$C = \frac{N_A \mu_{eff}^2}{3k}, \tag{2}$$

where C is the Curie constant, θ the Weiss temperature, N_A Avogadro's number, μ_{eff} the effective magnetic moment and k the Boltzmann constant. At temperatures below 20 and 100 K a significant deviation from a linear Curie–Weiss behaviour is observed for $LaHoO_3$ and $LaYbO_3$, respectively. This difference may be either attributed to crystal field effects on the $4f^N$ energy level or to exchange interactions in the RE^{3+} sublattice, the crystal field contribution being related to the crystal field components of the $^{2S+1}L_J$ levels of the RE^{3+} ions, that are unequally occupied at low temperatures.

The PM properties are interpreted in the general case of the Van Vleck theory applied to the rare-earth ions placed in the electrostatic potential of crystal field [9]. Detailed calculations of crystal field parameters related to the interpretation of magnetic results will be published elsewhere. The general method consists in determining the energy levels of the magnetic ions and then computing the disturbance made by the applied magnetic field H. In the case of rare-earth ions, the energy of spin–orbit coupling is mostly much greater than the energy due to the interaction with the electric field created

by the neighbour anions: the energy levels are then defined by the quantum number J and the crystal field removes the $2J+1$ degeneracy of level J. Owing to whatever interactions may be present, this state is split into a series of states $|n\rangle$ at energies E_n $(n = 1, \ldots, 2J+1)$.

Magnetic susceptibility is then given by

$$\chi_{\mathrm{M}} = \frac{N_{\mathrm{A}} g_J^2 \mu_{\mathrm{B}}^2}{kT} \left\{ \sum_n [|\langle n|J_z|n\rangle|^2 - 2 \sum_{n'} |\langle n|J_z|n'\rangle|^2 \times kT/(E_n - E_{n'})] \, \mathrm{e}^{-E_n/kT} \right\} \left\{ \sum_n \mathrm{e}^{-E_n/kT} \right\}^{-1}, \quad (3)$$

where the first term represents the direct contribution of level n to the susceptibility, responsible for the Curie behaviour, while the second one gives the 'induced' susceptibility which arises from admixtures of all the levels n' into n when an external field is applied (Van Vleck temperature-independent paramagnetism).

Whereas susceptibility rises steeply for $LaYbO_3$ and has appreciable high values, it barely varies with temperature for $LaHoO_3$ and its values are smaller. The insets of figures 1 and 2 show that there is minimal difference between the field-cooled (FC) and zero-field-cooled (ZFC) magnetizations. The lack of bifurcation between these two measurements appears to exclude the possibility of a spin glass state or any other frozen short-range ordered state above $T = 1.8$ K.

In the case of $LaYbO_3$ the n levels are not solely determined by crystal field interactions.

In $LaYbO_3$ the ground term of the free Yb^{3+} $(4f^{13})$ ion is $^2F_{7/2}$. A large spin–orbit coupling constant causes the lowest excited term, $^2F_{5/2}$, to lie at about 10 000 cm^{-1} above the ground term. Thus, the magnetic properties of ytterbium compounds are determined mainly by the splitting of the $^2F_{7/2}$ term in the crystal field [10]. The curves which represent the magnetic susceptibility as a function of temperature (figure 1, inset) show a sharp change of slope at about $T = 2.4$ K, as inferred from the derivative curve of magnetization (not shown), which presents a very sharp minimum at this temperature, in agreement with Ito *et al* reporting $T_{\mathrm{N}} = 2.7$ K [7]. In the temperature range between 300 and 100 K, χ^{-1} is linear, while a strong deviation from the Curie–Weiss law is observed at lower temperatures, mainly due to the thermal population effect. The value of the magnetic moment, calculated from the Curie constant in the linear region, is greater than that of the free ion Yb^{3+} $(4.93 \pm 0.02$ μ_{B} against 4.54 μ_{B}/fu theoretical). This difference can be explained by the fact that all crystal field levels are not occupied at these temperatures and the crystal field multiplet is very broad, since one has to reach a relatively high temperature, so that all the levels are equally populated. This behaviour has been reported for other Yb-containing compounds, such as Yb_2O_2S, for which the experimental Curie constant of the Yb^{3+} ion in the temperature range between 100 and 300 K for single crystal and powder samples is higher (4.8 μ_{B}) than the theoretical free ion value, following a Curie–Weiss law with a Curie constant corresponding to that of the free ion only for $T > 550$ K [11]. With decreasing temperature, the higher levels become depopulated, resulting in a susceptibility decrease, and the effective moment becomes temperature-dependent; at low temperatures only the ground doublet is occupied, but the exchange energy among Yb^{3+} ions becomes predominant, comparable to kT, and the compound orders. Consequently, it is necessary to take explicitly into account such interaction in the determination of the energy levels at the lowest temperatures. The calculated high-temperature PM Weiss temperature θ is -129.3 ± 1.4 K, suggesting antiferromagnetic ordering at low temperatures. The large difference between the value of θ and the Néel temperature T_{N} inferred from neutron data (2 K $< T_{\mathrm{N}} <$ 3 K, see section 3.2) for $LaYbO_3$ suggests that the main contribution to PM Weiss temperature comes from crystal field effects, whereas contribution from exchange interaction between Yb^{3+} ions plays a secondary role [12].

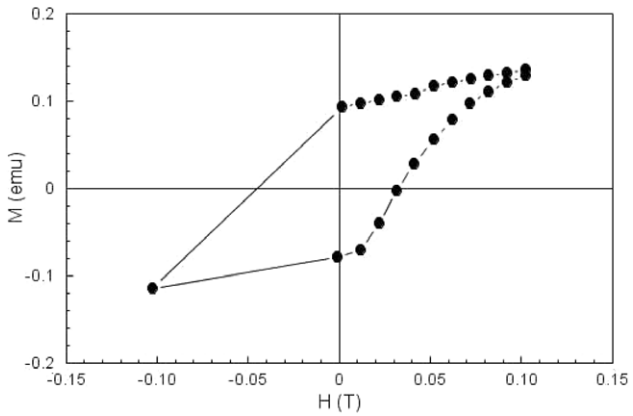

Figure 3. Magnetization as a function of magnetic field for $LaYbO_3$ sample at 1.8 K.

Magnetization measurements performed at 1.8 K (figure 3) show magnetic hysteresis indicative of a ferromagnetic ordering. Taking into consideration also the antiferromagnetic sign of the Weiss θ in the high-temperature range as previously mentioned and, secondly, that the magnitude of the M data (figure 1) appears to be too small (less than 0.5 emu mol^{-1} at the lowest temperature) to be attributed to a ferromagnetic moment, the existence of a ferromagnetic component in the magnetic properties of this compound can be inferred, as also confirmed from our neutron data discussion (see section 3.2).

$LaHoO_3$ magnetic susceptibility at high temperatures follows a Curie–Weiss type behaviour. The deviation from linearity observed at low temperature (below 20 K) can be attributed to the splitting of the free ion ground state under the influence of the crystal field where magnetic interactions can be neglected since no magnetic ordering has been observed down to 1.8 K.

Under these conditions Ho^{3+} ions behave on average as a set of free ions and their susceptibility can be calculated using the classical formula with

$$C = \frac{N_{\mathrm{A}} \mu_{\mathrm{B}}^2 g_J^2 J(J+1)}{3k}, \quad (4)$$

where g_J is the free ion Landé factor and J the quantum number corresponding to the fundamental level.

Table 1. Selected structural parameters and *R* factors of $LaYbO_3$ and $LaHoO_3$ obtained after Rietveld refinement of XRPD data collected at 300 K (space group: *Pnma*).

		$LaYbO_3$				$LaHoO_3$			
a (Å)		6.0301(1)				6.0945(1)			
b (Å)		8.4094(1)				8.5025(1)			
c (Å)		5.8360(1)				5.8817(1)			
Atom	Site	*x*	*y*	*z*	*B* (Å^2)	*x*	*y*	*z*	*B* (Å^2)
La	4c	0.0501(1)	$\frac{1}{4}$	0.9858(1)	0.11(1)	0.0506(1)	$\frac{1}{4}$	0.9846(1)	0.06(1)
Yb/Ho	4b	$\frac{1}{2}$	0	0	0.06(1)	$\frac{1}{2}$	0	0	0.38(1)
O(1)	4c	0.4528(2)	$\frac{1}{4}$	0.1189(2)	0.03(4)	0.4415(2)	$\frac{1}{4}$	0.1275(2)	0.09(3)
O(2)	8d	0.3124(2)	0.0625(1)	0.6903(2)	0.11(3)	0.3081(2)	0.0687(1)	0.6927(2)	0.21(3)
GII		0.15				0.18			
R_f (%)		4.49				5.54			
R_{Bragg} (%)		4.48				5.11			

The calculated Curie constant corresponds to a good approximation to the theoretical one for the free Ho^{3+} ion (theoretical $\mu_B = 10.60$; experimental $\mu_B = 10.75 \pm 0.01$) with $\theta = -6.5 \pm 0.4$ K. A rough estimate of exchange interactions can be obtained within the molecular field approximation from the Weiss temperature value obtained in the high-temperature limit when all crystal field states are occupied by [13]

$$\theta = \frac{2ZJ_{ex}J(J+1)}{3k}, \tag{5}$$

where J_{ex} is the exchange parameter, J the total angular moment and Z is the number of magnetic ions surrounding the Ho^{3+} ions. Taking $Z = 6$, we get $J_{ex}/k \cong 0.13 \pm 0.04$ K, thus showing that the antiferromagnetic coupling is very weak.

At low temperatures, moreover, the susceptibility tends to a constant value α (inset figure 2):

$$\chi = \frac{C}{(T-\theta)} + \alpha. \tag{6}$$

The Curie constant C is therefore zero, and this implies a singlet at a fundamental level.

3.2. Powder diffraction analysis and Rietveld refinement

XRPD and NPD analyses reveal that both $LaYbO_3$ and $LaHoO_3$ crystallize in the *Pnma* space group with a distorted perovskite-type structure at room temperature and retain this structure down to 1.5 K. Figure 4 shows the Rietveld refinement plot obtained for $LaYbO_3$ using the XRPD data collected at room temperature, revealing that the sample is constituted of a single-phase (structural data are reported in table 1).

From the structural point of view, in both $LaYbO_3$ and $LaHoO_3$ the octahedra coordinated by the RE element are significantly distorted and rotated with the same magnitude along the x and z axes of the pseudo-cubic cell with $a_p \sim a/\sqrt{2}$, $c_p \sim c/\sqrt{2}$ and $b_p \sim b/2$, but in opposite directions in adjacent layers; conversely, along the y axis they are rotated along the same direction. This octahedral tilting thus

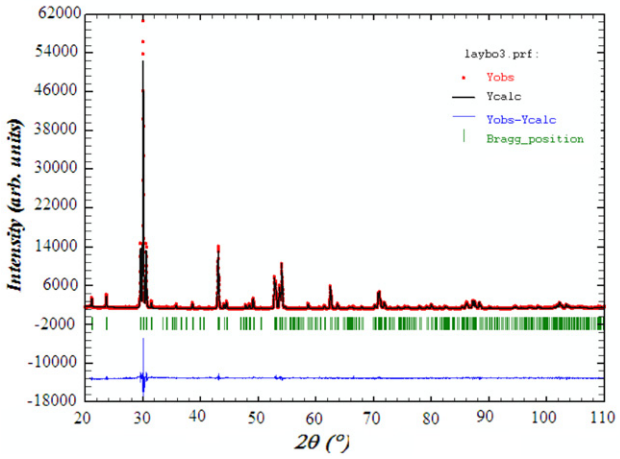

Figure 4. Rietveld refinement plot for $LaYbO_3$ (XRPD data collected at room temperature).

corresponds to the $a^-b^+a^-$ system (N. 10) proposed by Glazer [14]. In particular, tilting increases with the increase of the RE^{3+} ionic radius, being 19.6° and 21.3° along a, and 22.3° and 25.4° along b in $LaYbO_3$ and $LaHoO_3$, respectively. This behaviour clearly indicates that the ionic size of La^{3+} progressively becomes too small to sustain the corner connectivity among octahedra, with the consequent weakening of the perovskite-type structure stability as the RE^{3+} ionic radius increases, up to its suppression.

This is confirmed by bond valence sum (BVS) calculations [15], revealing that homologous sites exhibit about the same values in both compounds, except the RE^{3+} sites (table 2). In both compounds the La site is characterized by a notably lower BVS value than expected, indicating a stretched site. At the RE site a strong internal strain takes place in $LaHoO_3$, since its BVS exceeds the ideal value (3.00) of about 0.2 valence units (vu); conversely, the Yb^{3+} site is characterized by an almost optimal value. The root mean square of the BVS discrepancy for all the atoms can be a measure of the structural stability (GII: global instability index) [16, 17], playing a role similar to that of the

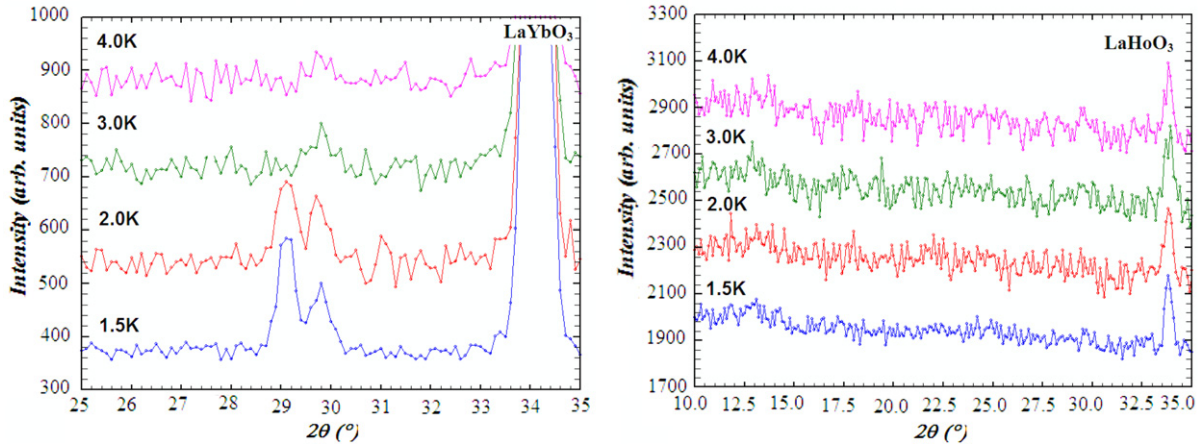

Figure 5. Enlarged view of the low-angle region of NPD patterns collected at low T. On the left: evolution of the AFM magnetic peaks in $LaYbO_3$; on the right: absence of magnetic peaks in $LaHoO_3$ down to 1.5 K.

Table 2. Bond valence sum and global instability index values of $LaYbO_3$ and $LaHoO_3$ obtained from the structural parameters of table 1.

	BVS (vu)	
Atom	$LaYbO_3$	$LaHoO_3$
La	2.73	2.70
Yb/Ho	2.97	3.18
O(1)	1.94	1.99
O(2)	1.88	1.94
GII	0.15	0.18

Goldschmidt tolerance factor. As a rule, the structure becomes unstable under normal conditions when large internal strains induce GII values higher than 0.2 vu. As already mentioned, in $LaHoO_3$ the RE site undergoes a notable strain that increases the GII up to a limit value (table 2); hence it is expected that a further increase of the RE ionic radius should determine an instability of the perovskite-type structure, as is actually observed in the case of $LaDyO_3$ [5].

Structural data obtained at 1.5 K (table 3) from NPD analysis reveal that both compounds exhibit a negative thermal expansion along the a and b axes, driven by the cooperative tilting of the octahedra on cooling.

NPD patterns of $LaYbO_3$ collected between 1.5 and 4 K evidence the arising of relatively strong AFM peaks between 2 and 3 K (figure 5, on the left), in the temperature range where a sharp slope change is observed in the magnetic susceptibility curves; note that the weak scattering around 29.7° 2θ at $T > 3$ K is originated by the faint 011 nuclear peak. These magnetic peaks are characterized by a commensurate magnetic wavevector $\mathbf{q} = (0\,0\,0)$.

Rietveld refinement (figure 6; structural data are reported in table 3) reveals that the Yb sublattice orders according to a G_z-type structure, belonging to the $Pn'ma'$ magnetic space group. The ordered magnetic moment for this spin component is strongly reduced, resulting in 0.82(3) μ_B.

As detected in our magnetization measurements and reported by Ito *et al* [7] as well, a weak ferromagnetic

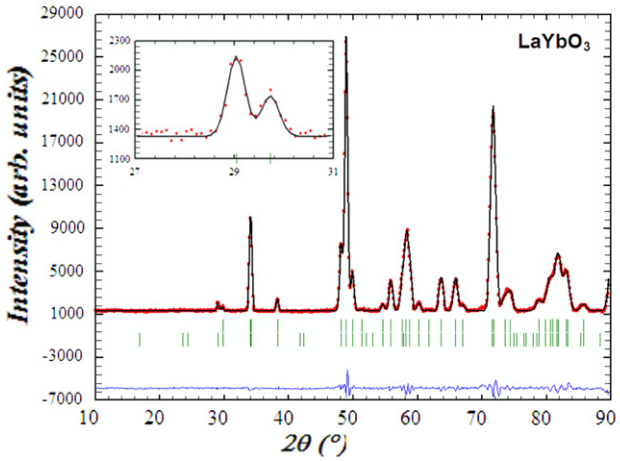

Figure 6. Rietveld refinement plot obtained for $LaYbO_3$ (NPD data collected at 1.5 K); the inset shows an enlarged view in the angular region of the G_z AFM peaks.

component should also be present. A closer analysis of the NPD patterns reveals a very faint increase of the scattered intensities at the 101 and 121 peak positions (figure 7) at 1.5 K, that could be possibly related to a F_y-type spin ordering, belonging to the same $Pn'ma'$ magnetic space group. The insets of figure 7 show that the increased intensity observed at lower temperature significantly exceeds the experimental uncertainty, corroborating the scenario foreseeing the presence of a faint ferromagnetic ordered component. A net decrease of the magnetic R-factor (from 8.42% down to 7.98%) is obtained when this magnetic component is taken into account in Rietveld refinements. On the other hand, the refined FM moment has about the same value of the calculated error; in fact, for the F_y-type spin ordering the ordered magnetic moment results in 0.3(3) μ_B. By applying the significance test on the magnetic R-factors [18], the hypothesis that the F_y magnetic component must be neglected can be rejected at the 0.250 level; hence this component in the NPD pattern is more likely to occur than not, even though the confidence level is quite low.

Table 3. Selected structural parameters and *R* factors of $LaYbO_3$ and $LaHoO_3$ obtained after Rietveld refinement of NPD data collected at 1.5 K (space group: *Pnma*).

		$LaYbO_3$			$LaHoO_3$		
a (Å)		6.0327(1)			6.0964(1)		
b (Å)		8.4138(1)			8.5235(2)		
c (Å)		5.8307(1)			5.8738(1)		
Atom	Site	*x*	*y*	*z*	*x*	*y*	*z*
La	4c	0.0499(1)	$\frac{1}{4}$	0.9859(1)	0.0523(1)	$\frac{1}{4}$	0.9874(1)
Yb/Ho	4b	$\frac{1}{2}$	0	0	$\frac{1}{2}$	0	0
O(1)	4c	0.4455(1)	$\frac{1}{4}$	0.1235(1)	0.4388(1)	$\frac{1}{4}$	0.1350(1)
O(2)	8d	0.3062(1)	0.0647(1)	0.6929(1)	0.3050(1)	0.0625(1)	0.6908(1)
μ_{Yb} (μ_B)		0.87(13)			—		
R_f (%)		1.91			5.33		
R_{Bragg} (%)		1.23			7.42		
$R_{Magnetic}$ (%)		7.98			—		

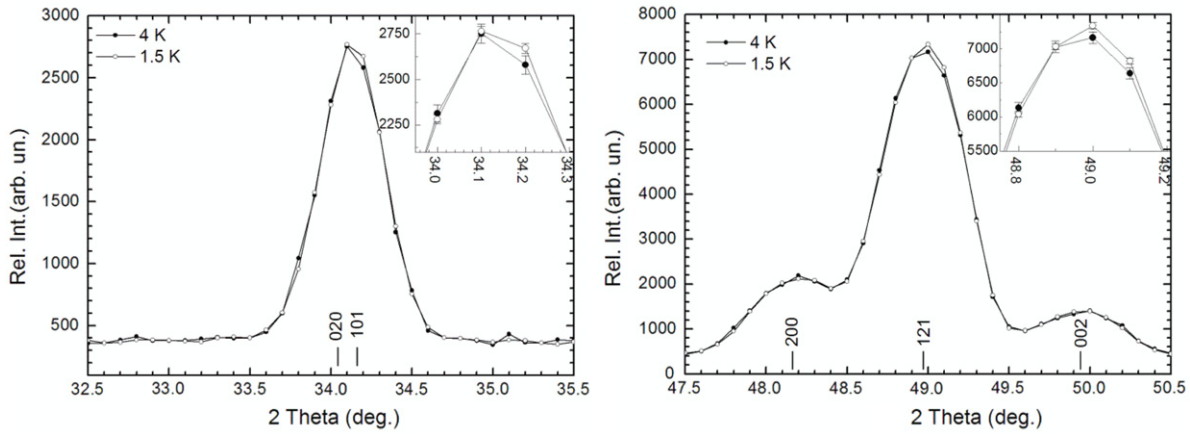

Figure 7. Superposition of the NPD patterns of $LaYbO_3$ collected at 1.5 and 4 K in the regions where a faint increase of the scattered intensity is observed at lower temperature, possibly originated by the onset of a F_y-type spin ordering; the insets show an enlarged view of the peaks evidencing that the increased intensity exceeds the experimental error.

Even though any firm conclusion is prevented by its weakness, several experimental evidences corroborate the occurrence of the F_y-type spin ordering component: (1) the magnetic hysteresis arising in the magnetization measurements performed at 1.8 K; (2) the significant faint increase of the neutron scattering at the position expected for a F_y-type spin ordering, exceeding the experimental uncertainty; (3) the significant decrease of the magnetic *R*-factor in Rietveld refinement when the F_y-type component is taken into account in the structural model.

The magnetic structure of $LaYbO_3$ can thus be described as a F_yG_z-type spin ordering, belonging to the $Pn'ma'$ magnetic space group, with a total magnetic moment of 0.87(13) μ_B (figure 8), in agreement with magnetization measurements. Noteworthy is that Yb^{3+} spins are canted, as argued by Ito *et al* [7], and lie in the equatorial planes of the octahedra.

In the NPD patterns of $LaHoO_3$ no magnetic peak can be detected and the compound appears PM down to 1.5 K (figure 5, on the right). This is in agreement with the fact that Ho^{3+} has even paired electrons ($4f^{10}$), whereas Yb^{3+} is a Kramers ion with odd unpaired electrons ($4f^{13}$). Structural data for $LaHoO_3$, as obtained from Rietveld refinement of the NPD data collected at 1.5 K, are reported in table 3. Because of the rather large thermal absorption cross section of Ho, the ratio between the coherent and incoherent neutron scattering in the NPD patterns of $LaHoO_3$ is strongly reduced; as a consequence the goodness of the Rietveld refinement, although acceptable, decreases as well (table 3).

The magnetic properties of $LaYbO_3$ and $LaHoO_3$ are thus different from what was obtained by Moreau *et al* for $LaErO_3$ [6]: in that case spins order at low *T* (T_N = 2.4 K), but according to an $A_xG_yC_z$-type structure, belonging to the *Pnma* magnetic space group, with a total magnetic moment equal to 6.34 μ_B. Moreover, $LaErO_3$ exhibits metamagnetism below 4 K [19], whereas in $LaYbO_3$ no evidence for this phenomenon has been ascertained down to 1.8 K [7].

4. Conclusions

Both $LaYbO_3$ and $LaHoO_3$ crystallize in an orthorhombic perovskite-type structure, isostructural with $GdFeO_3$ between

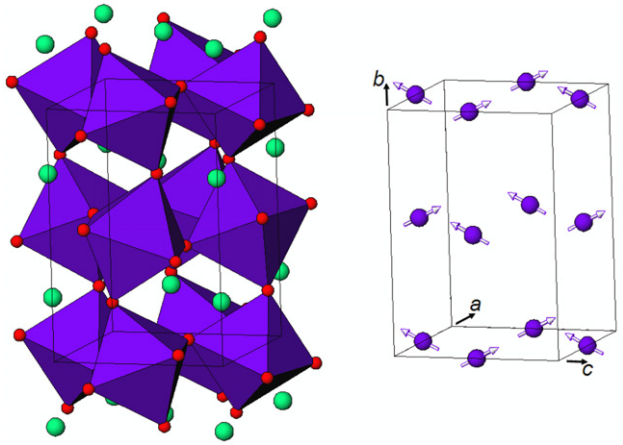

Figure 8. Crystal structure of $LaYbO_3$ and F_yG_z-type spin ordering of the Yb^{3+} ions at 1.5 K. (Yb at the octahedral site; O at the octahedral corners; La in the voids of the corner-shared octahedral framework.)

1.5 and 300 K, and are characterized by negative thermal expansion along the *a* and *b* axes.

Magnetic ordering of Kramers ion Yb^{3+} in $LaYbO_3$ is made possible because the ground crystal field level is a Kramers doublet. As for non-Kramers ion Ho^{3+}, magnetic ordering is only possible if the ground level is a doublet, which is usually not the case when the point symmetry of the RE^{3+} site is low, as in $LaHoO_3$, and the magnetic interaction is weak.

In rare-earth compounds, ions with even number of electrons may have singlet ground-state levels. However, this does not necessarily prevent such a system from having magnetic ordering at low temperatures. It has been demonstrated that, when the exchange interaction exceeds a certain critical value relative to the crystal field, a magnetic ordering occurs in a low-temperature region.

According to the results derived from susceptibility analysis, the crystal field ground levels of Ho^{3+} ions are all singlet levels.

This scenario is confirmed by neutron powder diffraction analysis, revealing that $LaYbO_3$ is characterized by a F_yG_z-type ordering of the Yb^{3+} spins below 2.4 K, with spins lying in the equatorial plane of the octahedra; conversely, $LaHoO_3$ is paramagnetic down to 1.5 K.

Deviations from linearity in the magnetic susceptibility curves observed at low temperatures can be attributed to the splitting of the free ion ground state under the influence of the crystal fields and the calculated Weiss constants are entirely due to crystal field effects for $LaHoO_3$, since it does not undergo magnetic ordering; different is the case for $LaYbO_3$, for which exchange interactions and thermal population effects are simultaneously present. Moreover, the crystal field contribution has a different role in the Weiss temperature values observed, contributing a large part where dominant.

However, possible effects linked to structural changes must be also taken into account: with decreasing size of RE^{3+} ion, the RE–RE distance decreases, leading to a looser packing.

That means that a detailed and complete crystal field strength analysis would require information from PM susceptibility connected with the distribution of the first crystal field levels deduced from inelastic neutron scattering or specific heat measurements, completed with a model for calculating crystal field parameters from crystallographic positions.

References

[1] Berndt U, Maier D and Keller C 1975 *J. Solid State Chem.* **13** 131
[2] Bharathy M, Fox A H, Mugavero S J and zur Loye H C 2009 *Solid State Sci.* **11** 651
[3] Ovanesyan K L, Petrosyan A G, Shirinyan G O, Pedrini C and Zhang L 1998 *Opt. Mater.* **10** 291
[4] Goldschmidt V M 1926 *Naturwissenschaften* **14** 477
[5] Artini C, Costa G A, Carnasciali M M and Masini R 2010 *J. Alloys Compounds* **494** 336
[6] Moreau J M, Mareschal J and Bertaut E F 1968 *Solid State Commun.* **6** 751
[7] Ito K, Tezuka K and Hinatsu Y 2001 *J. Solid State Chem.* **157** 173
[8] Rodríguez-Carvajal J 1993 *Physica* B **192** 55
[9] Van Vleck J H 1932 *The Theory of the Electric and Magnetic Susceptibilities* (London: Oxford University Press)
[10] Huang Q, Wang Q, Chang J, Zhang X and Liu Z 2009 *Proc. SPIE* **7630** 76301B
[11] Quezel G, Ballestracci R and Rossat-Mignod J 1970 *J. Phys. Chem. Solids* **31** 669
[12] Paradowski M L, Pacyna A W, Bombik A, Korczak W and Korczak S Z 2000 *J. Magn. Magn. Mater.* **212** 381
[13] Anderson P W 1963 *Solid State Physics* vol 14, ed F Seitz and D Turnbell (New York: Academic) p 99
[14] Glazer A M 1975 *Acta Crystallogr.* A **31** 756
[15] Brown I D and Altermatt D 1985 *Acta Crystallogr.* B **41** 244
[16] Rao G H, Bärner K and Brown I D 1998 *J. Phys.: Condens. Matter* **10** L757
[17] Salinas-Sanchez A, Garcia-Muñoz J L, Rodriguez-Carvajal J, Saez-Puche R and Martinez J L 1992 *J. Solid State Chem.* **100** 201
[18] Hamilton W C 1965 *Acta Crystallogr.* **18** 502
[19] Moreau J M 1969 *Mater. Res. Bull.* **3** 427